ACCURACY ISSUES IN EXPERIMENTAL STUDIES OF TILT SENSORS

Sergiusz Łuczak*

Problems related to accuracy of tilt measurements realized during experimental studies of miniature tilt sensors (including MEMS devices) are minutely discussed. The measurements are performed by means of a custom computer controlled test rig, over the full range of pitch and roll. Accuracy of the test rig is determined in terms of uncertainty of the measurements involved. Ways of improving performance of the test rig are briefly introduced. Exemplary results of experimental works are presented.

Keywords: *test rig, tilt sensor, accuracy, experimental studies*

1. Introduction

In many cases, when metrological parameters of a sensor are of a high importance, it is necessary to subject it to appropriate experimental studies. Generally, such situation takes place when:

- significant metrological parameters of a sensor are not provided (prototype sensors, like in [1]–[2]; insufficient information in the relevant catalogs),
- value of important metrological parameters of a sensor may be overestimated in the catalog (e.g. due to a high variability of the fabrication process like in the case of MEMS accelerometers referred to in [3]–[7]),
- a sensor must be calibrated by the user, like in the case of most MEMS sensors, e.g. accelerometers referred to in [3]–[6],
- an improvement of the sensor performance is striven for (e.g. by the way of compensating for the systematic errors, like cross-axis sensitivity or misalignment of the sensitive axes), as in [8],
- significance of interactions between the accuracy and some disturbances must be verified,
- results of aging of a sensor must be determined,
- improvement in performance of a sensor must be verified,
- durability or stability of a sensor must be determined.

At times, some experimental studies, especially calibration of a sensor, can be realized without a test rig, during a standard operation of the device that contains the concerned sensor. However, a complicated theoretical model of the sensor operation must be usually developed then, and lower accuracy is to be taken into account.

As far as measurements of the tilt are concerned (which can be useful while operating many various systems, e.g. pan and tilt device presented in [9]) they are realized often with

* Eng. S. Łuczak, Ph.D., Division of Design of Precision Devices, Institute of Micromechanics and Photonics, Faculty of Mechatronics, Warsaw University of Technology, ul. Boboli 8, 02-525 Warsaw, Poland

low-range MEMS accelerometers, such as those referred to in [3]–[7], despite the fact that their accuracy is much lower compare to their conventional counterparts. Then, the only way to obtain values of the parameters better than those reported in the catalog data is to perform appropriate experiments, where two pivotal issues are methodology of performing the experiments and the related test rig, whose precision significantly influences the results to be obtained. Sometimes an adapted universal test rig can be used in order to carry out experimental studies of a tilt sensor [10]–[17]. In other cases, a custom test rig must be constructed, like in [18], [19]. It was just the case when the author was working on a miniature tilt sensor to be applied in a snake-like microrobot described in [20]. The experiments have been carried out using an initial version of a test rig described in [21], [22]. Its fully developed structure has been presented later in the text.

The test rig being described must have met the following basic technical requirements:

- applying angular position of the tested sensor over the steregon (i.e. over 360° around two horizontal and perpendicular axes) with accuracy no lower than 1.2 minute arc (0.02°),
- reading indications of the tested sensor by measuring its analog output voltages with accuracy no lower than 0.005 V,
- recording the applied angular positions of the tested sensors with its corresponding indications in the computer memory,
- performing automatically series of measurements over a chosen angular range with a given resolution.

The accepted values of the accuracies result from the accuracy of the tested MEMS sensors, foreseen as the basic kind of sensors to be tested, reported in the catalog data (assuming that the accuracy of a measuring instrument should be at least 10 times higher than the measurand itself). Although the accuracy of 6 minutes arc (relative value of 0.03 % as referred to the measuring range) is sufficient for MEMS devices, it may be too low in the case of conventional tilt sensors (e.g. sensitive liquid sensors with a small measuring range). So, the presented test rig features also higher accuracy while applying the pitch angle.

2. The geometrical relationships

Although the considered test rig can be used for studying various kinds of tilt sensors, further considerations will be limited to accelerometer-based tilt sensors only.

It has been commonly accepted that tilt is represented by two components: pitch and roll [23]. Therefore, the test rig should make it possible to apply pitch and roll directly. Fig. 1

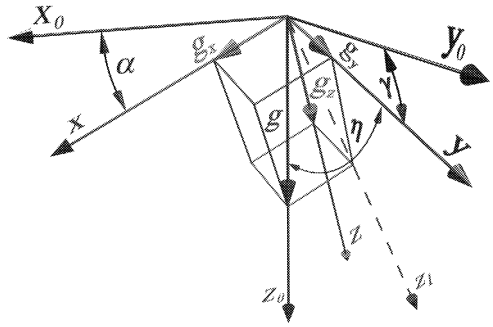

Fig.1: Tilt angles applied by means of the test rig

illustrates the respective kinematics of the test rig, where: α – pitch angle, γ – roll angle, η – complement of angle β indicated by the tested sensor [24], g – gravitational acceleration, g_x, g_y, g_z – Cartesian components of the acceleration g. The coordination system $x_0y_0z_0$ is immovable, and the axis z_0 overlaps direction of the gravitational acceleration. The coordination system xyz is attached to the tested tilt sensor. At the initial position axes of both systems overlap each other.

Operation of the test rig can be described as follows. A chosen angular position is approached in two steps. First, the tested sensor is rotated around the horizontal axis y_0, and thus a pitch angle α is applied. As a result, positions of axis x and z change. The later will be located in an intermediate position designated as z_1. Axis y still overlaps axis y_0. The respective output signal of the tested sensor changes then according to the following formula:

$$g_x = g \sin\alpha \ . \tag{1}$$

Subsequently, the sensor is rotated around the axis x (which has been relocated from its initial horizontal position) and in this way a roll angle γ is applied. As a result, axis y relocates from position y_0 and axis z from the intermediate position z_1. Since the rotation took place around axis x, the output signal corresponding to the acceleration component related to this axis does not change, while the other two output signals of the tested sensor can be determined as follows:

$$g_y = g \cos\eta = g \sin\beta \ , \tag{2}$$

$$g_z = g \cos\alpha \cos\beta \ . \tag{3}$$

With regard to the value of acceleration component g_y in direction y, it should be noted that axis y and y_0 create a plane yy_0 tilted by angle α with respect to the vertical, i.e. axis z_0. Therefore, the acceleration component on axis y (determined by angle β) will be dependent both on angle α as well as γ. It is shown in Fig. 2.

As it results from Fig. 2:

$$g_y = g_\alpha \sin\gamma = g \cos\alpha \sin\gamma \ . \tag{4}$$

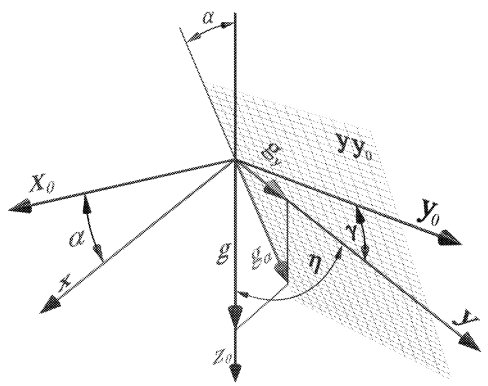

Fig.2: The components of the gravity vector against pitch α and roll γ

By combining Eq. (2) with (4) we can obtain a dependence allowing us to determine value of angle β (indicated indirectly by the tested sensor), while knowing values of pitch α and roll γ applied by means of the test rig:

$$\beta = \arcsin(\sin\gamma \cos\alpha) \ . \tag{5}$$

A graphical interpretation of the above formula is presented in Fig. 3. (It should be noted that occurrence of the acute peaks results from computation limitations due to the fact that the range of the arc sine function is of $\langle -90°; 90° \rangle$, and while generating the graph the computer instead of increasing value of angle β over 90° had changed it stepwise to −90° and only then increased it.)

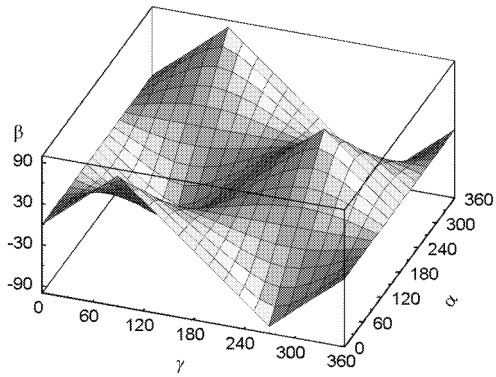

Fig.3. Dependency of angle β on pitch α and roll γ

As can be observed in Fig. 3, for angles α other than 0°, 180° and 360° variations of angle β as a function of angle γ are diminished (for angles α of 90° or 270°, angle β equals 0° regardless to the values of angle γ). It must not be overlooked that in a general case, it is impossible to apply any arbitrary combination of angles α and β, indicated by the tested sensor, as these are interrelated – one affects the other.

In conclusion, an advantage of the accepted geometrical structure of the test rig is its simplicity and facility of practical realization. However, a shortcoming consists here in a necessity of computing the applied tilt angles in order to compare them with indications of accelerometer-based tilt sensors. Such processing results in variations of the uncertainty of determining the angular position of the tested sensor, what is discussed in section 4.1.

3. The test rig

The test rig, schematically shown in Fig. 4, consists of four modules – two universal and two custom-designed.

The universal modules are:

- a PC with an analog-digital data acquisition card (e.g. Advantech PCL 818L), operating under Windows system, and running a driver software that controls the test rig (developed in Visual Basic environment),
- an electronic counter AE 101 coupled with an incremental angle transducer IDW 2/16384 manufactured by Jenoptik Carl Zeiss JENA, attached to the mechanical module.

The custom modules are:

- a mechanical structure consisting of two rotary tables powered by stepper motors, a bed made of cast iron, mechanical elements integrating the rotary tables, a special aligning holder of the tested sensor, a supporting footstock, and spirit levels (for leveling the bed),
- an electronic module containing drivers of the stepper motors, a logic circuit controlling the drivers, and transducers coupled with position sensors in the rotary tables.

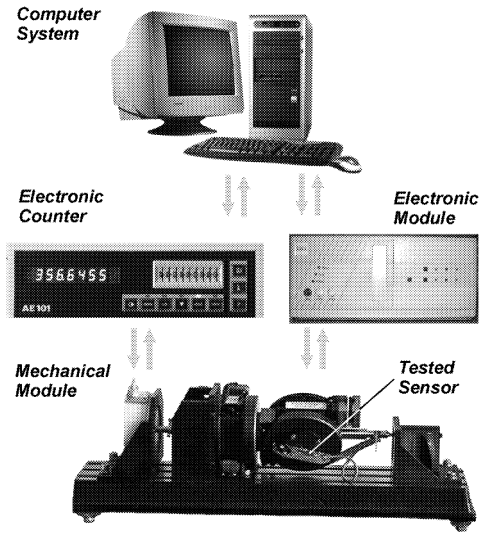

Fig.4: The test rig

The test rig operates in the following way. The driver software communicates with the electronic module via the analog-digital data acquisition card. Next, the electronic module actuates the mechanical structure (along with the tested sensor), applying a desired angular position of the rotary tables. Then, the analog output signals from the tested sensor are collected by the analog-digital data acquisition card and recorded in a file against the corresponding real angular positions of the rotary tables (resulting from calculated positions of the tables and additionally indicated by the incremental angle transducer). Comparison of these two sets of data in a further processing is one of the ways of evaluating accuracy of the tested sensor.

The above sequence of operations may be repeated automatically within a chosen angular range with a desired step, thus the full measurement range of pitch and roll can be covered.

The mechanical module of the test rig has been designed in such a way that its geometrical configuration allows the tilt to be applied as its two components: pitch and roll, as discussed in section 2. It also makes it possible to apply any angular position of the tested sensor over the steregon with a satisfactory accuracy. The main members of this module, presented in Fig. 5, are two rotary tables 1 and 2 powered by stepper motors driving their top through a worm gear. Resolution of the tables is of $1.2'$ ($0.02°$). They are equipped with special optical sensors indicating initial position of the top.

The stationary table 1 applies the pitch angle α while the moveable table 2 applies the roll angle γ. The tested sensor 3 is fixed to the moveable table by means of an aligning holder.

The stationary table 1 is additionally connected with the incremental angle transducer, thus inaccuracies of its components do not influence accuracy of determining value of the applied angular position, since it is dependent only on the accuracy of the transducer and the employed coupling. The resultant higher accuracy is necessary in some cases, especially while testing precise tilt sensors, usually with a small measuring range (operating as leveling devices), and thus featuring high absolute accuracy.

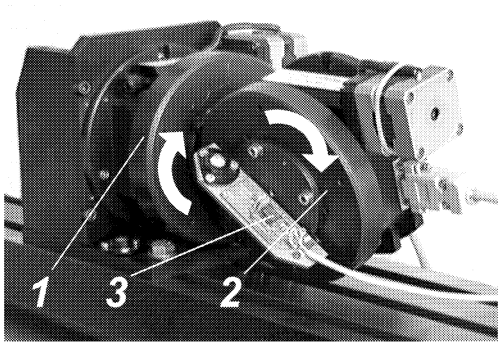

Fig.5: The rotary tables: 1 – stationary table, 2 – moveable table, 3 – tested sensor

The computer sets a given angular position of the rotary tables in two steps. First, the stationary table is activated, and it rotates along with the movable table, which is not powered. Then, the movable table is activated, while the angular position of the stationary table is kept. As the stationary table is connected with the angle transducer (see Fig. 4) by means of a precise coupling, it is possible to determine position of the table with a high accuracy of ca. 1.5 seconds arc.

The pitch angle is applied by means of the stationary table (its rotation axis is always horizontal), while the roll angle is applied by means of the movable table (fixed to the first table; its rotation axis gets tilted as pitch is applied). Because deflection of the rotary shaft of the stationary table caused by the weight of the moveable table and the integrating elements was of few minutes arc, the test rig has been equipped with a special footstock (see Fig. 4) supporting the rotation axis of the stationary table.

Methodology of performing the experimental studies by means of the test rig is briefly addressed later in the text.

4. Evaluation of the accuracy of the test rig

The accuracy of the test rig refers to two issues:

– accuracy of applying angular position (pitch and roll) of the tested sensor,
– accuracy of reading the output analog voltages of the tested sensor.

It should be noted that evaluated values of the aforementioned accuracies significantly influence the experimental results obtained while testing tilt sensors. Knowledge of their values is imperative before starting the experimental studies, as accuracies of the test rig must be always higher (at least of one order) than the expected accuracy of the sensor to be tested.

It was decided to evaluate the accuracy on the basis of respective uncertainties of measurements involved, representing the random errors.

4.1. Uncertainty related to the computed tilt angles

The test rig makes it possible to apply an arbitrary angular position (i.e. pitch and roll) over the entire range of indications of tilt sensors with a constant uncertainty resulted from uncertainty of the rotary tables and the angle transducer.

However, in order to verify uncertainty of the tested sensor, angles α and β must be first determined using rearranged Eq. (1)–(3). Then, they must be compared with the pitch and the roll applied by means of the rotary tables. In the case of angle α this can be accomplished directly, so the respective uncertainty results from uncertainty of the incremental angle transducer (or uncertainty of the rotary table, when the test rig operates in an open loop mode). Yet, in the case of angle β, the applied pitch and roll angles must be combined on the basis of Eq. (5). This results in a variable uncertainty of determining the applied angle β.

According to the guidelines of the International Organization for Standardization, we can use the following general formula derived from [25] to determine a combined standard uncertainty of applying roll:

$$u_{\mathrm{c}}(\beta) = \sqrt{\left(\frac{\partial \beta}{\partial \alpha}\, u(\alpha)\right)^2 + \left(\frac{\partial \beta}{\partial \gamma}\, u(\gamma)\right)^2} \tag{6}$$

where $u(\beta)$ is combined uncertainty of angle β; $u(\alpha)$, $u(\gamma)$ – standard uncertainty of the respective rotary table.

By substituting Eq. (5) to (6), we obtain the following equation:

$$u_{\mathrm{c}}(\beta) = \sqrt{\left(\frac{\sin\alpha\, \sin\gamma}{\sqrt{1-\cos^2\alpha\, \sin^2\gamma}}\, u(\alpha)\right)^2 + \left(\frac{\cos\alpha\, \cos\gamma}{\sqrt{1-\cos^2\alpha\, \sin^2\gamma}}\, u(\gamma)\right)^2}\,. \tag{7}$$

Since the rotary tables are of the same type, for further analyses we can accept an initial assumption that:

$$u(\alpha) = u(\gamma) \tag{8}$$

and in this way, obtain a reduced form of Eq. (7):

$$u_{\mathrm{c}}(\beta) = u(\alpha)\sqrt{\frac{\cos^2\alpha\, \cos^2\gamma + \sin^2\alpha\, \sin^2\gamma}{1-\cos^2\alpha\, \sin^2\gamma}}\,. \tag{9}$$

A graphical interpretation of Eq. (9) over the full domain of angles α and γ is presented in Fig. 6. Numbers over axis y are values of the combined standard uncertainty of determining angle β for $u(\alpha) = 1$ (the first term of Eq. (9) on the right).

As can be observed, the considered uncertainty does not exceed the uncertainty related to operation of the rotary tables $[u(\alpha) = u(\gamma)]$ over the whole measuring range of the test rig. The minimal values of the considered uncertainty, i.e. of zero or near-zero, correspond to insignificant values of the angle itself. Thus, generally, the uncertainty of determining angle β will approximately equal uncertainty of determining angle α. In other words, it can be stated that computing angle β according to Eq. (5) does not result in increase of the respective uncertainty. It should be also noted that Eq. (9) reaches all the possible values

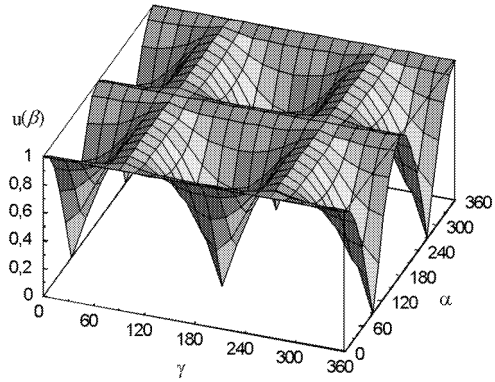

Fig.6: Variations of the uncertainty of determining angle β

for angles α and γ varying over the range of $\langle 0°; 90°\rangle$. However, it must be realized that determining roll γ on the basis of the indications of the tested sensor results in a significant increase of the related uncertainty.

4.2. Uncertainty related to the data acquisition card

The uncertainty of measuring the analog output voltages of the tested sensor results from parameters of the applied data acquisition card, in this case Advantech PCL 818L. According to a related datasheet [26], the relevant parameters are as follows:

- resolution of the A/C converters: 12 bits,
- accuracy of reading the input voltage: 0.02 % of the full scale range ±1 bit (i.e. 1/4096) of this range.

On a basis of the tests that had been realized beforehand, it was foreseen that the following ranges of the input voltage U would be used: 5; 2.5; 1.25 V (depending on the range of the output voltages generated by the tested sensors).

Regarding the above data, uncertainty of measuring the input voltage U by means of the applied card can be determined. Two factors are decisive here, both dependent on the accepted range of the input voltage $U_{\max}$. Since [26] defines only an interval (0.02 % $U_{\max}$), where the error of reading the output voltage can be found, with no additional information, it should be assumed that we deal in this case with a uniform distribution of the possible values [25]. The second factor determining the uncertainty of reading the voltage is connected with the resolution of the card. In this case we also deal with a uniform distribution [25].

For the uniform distribution, the uncertainty $u(U)$ can be calculated according to the following formula derived from [25]:

$$\begin{aligned} u_{\mathrm{c}}(U) &= \frac{1}{\sqrt{3}} \sqrt{(0.0002\, U_{\max})^2 + \left(\frac{U_{\max}}{2^{12}}\right)^2} \approx \\ &\approx \frac{1}{\sqrt{3}} \sqrt{(0.00020\, U_{\max})^2 + (0.00024\, U_{\max})^2} \approx 0.00018\, U_{\max} \,. \end{aligned} \tag{10}$$

It should be noted that the component related to the resolution is more significant here. So, it is reasonable to use a data acquisition card with 14-bit or 16-bit A/D converters.

In the case of the widest range of the measured voltages (i.e. 0–5 V) [full scale range is then ($U_{\max} = 5\,\mathrm{V}$)], we obtain the maximal value of the uncertainty of measuring the voltage $u_{\mathrm{c}}(U) = 0.0009\,\mathrm{V}$. We can calculate also an expanded uncertainty. For a uniform distribution, the coverage factor k_{p} will be of 1.71 at the confidence level $p = 99\,\%$ [25], so value of the expanded uncertainty will equal $U(U) = 0.0016\,\mathrm{V}$.

In the case of a necessity of using more accurate 16-bit cards, e.g. PCI 1741 by Advantech, the expanded uncertainty will be of 0.0010 V. Such necessity may result e.g. from the fact that the traditional approach of using a measuring device with accuracy 10-times higher than the measurand itself, may not be satisfactory. If the obtained measurement results are to be statistically processed in further steps, it is expected that they will be compliant with the normal distribution. If their scatter is too small (due to low accuracy of the measuring instrument), the hypothesis regarding the normal distribution cannot be proved, what significantly complicates further statistical analyses.

Apart from applying a more accurate data acquisition card, uncertainty of measuring the output signals of the tested sensor can be decreased in two other ways. In some cases it is sufficient to eliminate the offset of the output signal generated by the tested sensor (what is usually the case with MEMS accelerometers, e.g. sensors referred to in [3]–[7]). Then, we can decrease the input range of the card, and thus obtain a higher resolution of the measured voltage (up to 16-times higher in the case of the applied card PCL 818L) as well as smaller value of the relevant uncertainty [see Eq. (10)]. The simplest way to realize it is to use a reference voltage, having value similar to the sensor offset, and employ differential analog inputs of the card, instead of the single-ended inputs. Another approach is to apply some operational amplifiers, compensating the output voltage of the sensor for the offset. However, in this case some loss of accuracy of the measured voltage must be taken into consideration. Still another solution is to use a reference voltage generated by some MEMS sensors, e.g. MXA 2500 by MEMSIC Inc. [7]. However, tests performed by the author revealed that this voltage is very unstable, with variation of ca. 0.01 V.

As far as MEMS accelerometers are concerned, many of them generate digital output signals, even though their principle of operation has an analog character. It is easier to read digital signals with a PC, yet a computer data acquisition card is usually much more accurate than the digital circuits integrated with the MEMS accelerometer. Still another concern is resolution of the circuits, which is usually too low for research purposes, e.g. 8 bits. So, generally, while studying MEMS accelerometers it is better to use their analog output signals.

4.3. Uncertainty related to operation of the rotary tables

In order to evaluate uncertainty related to both rotary tables, appropriate tests were carried out. Values of their angular displacements were verified by means of the incremental angle transducer (rotation-to-pulse sensor) IDW 2/16384 by Jenoptik Carl Zeiss JENA that was connected with the electronic counter AE 101 processing its output signals. The angle transducer was coupled with the tested tables by means of a precise coupling. In both cases, the respective configuration was the same as in Fig. 4 with regard to the stationary table.

While determining positioning errors of the tables the following values of the mutual misalignment of the interconnected shafts (the output shaft of the angle transducer and the output shaft of the table) were not exceeded : radial run-out of the table output shaft of 0.06 mm;

coaxiality error of 0.01 mm; twist of the axes of 0.046°. Values of the listed errors significantly influence accuracy of the coupling used for connecting the tested table with the angle transducer [27]–[28], so it was striven for obtaining possibly low values of these errors.

In the case of the tests of the stationary table, a precise flexible coupling PF type by Jenoptik Carl Zeiss JENA was used, whereas the moveable table, because of lack of space, had to be connected with the angle transducer by means of a bellows coupling, for this kind of coupling features the highest accuracy among the couplings easily available [27].

According to the relevant datasheet, measurement errors of angular positions realized by means of the angle transducer can be found within an interval of a length $a = \pm 1$ second arc [29], whereas the error related to operation of the applied couplings was hard to be estimated.

In the case of the stationary table, the manufacturer declares that the possible values of the error of the flexible coupling used (PF type) cover an interval of a length $c = \pm 1$ second arc [29]. So, the combined uncertainty $u_c(\alpha)$ of measuring the angular position applied by this table, accepting as previously a uniform distribution of the component uncertainties [25], can be calculated according to a formula analogous to Eq. (6) and (10):

$$u_c(\alpha) = \frac{1}{\sqrt{3}} \sqrt{a^2 + c^2} \approx 0.82\,\text{sec} \approx 0.00023\,\text{deg} \,. \tag{11}$$

Accepting again the coverage factor k_p of 1.71, value of the expanded uncertainty will equal $u_c(\alpha) \approx 1.4''$. Since the angle transducer is coupled with the stationary table during a standard operation of the test rig, so accuracy of applying pitch can be also evaluated at ca. 1.5 seconds arc (ca. 0.0004°).

In the case of the moveable table, the related literature estimates accuracy of the bellows coupling applied in the tests at ca. 50 seconds arc [25]. (Despite such significant difference between the coupling accuracy referred to, no radical difference has been observed in the characteristics of the rotary tables obtained while using both kinds of the couplings, what suggests that accuracy of the bellows coupling must have been in fact higher.) Using Eq. (11) and accepting the confidence level $p = 99\,\%$, it can be calculated that the positioning errors of the second table have been determined with expanded uncertainty of 50 seconds arc (0.007°).

The uncertainty related to operation of the tables results from kinematic errors of its components: the stepper motor, the worm gear, the coupling connecting the motor with the gear and the bearings supporting the gear shafts. In order to evaluate this uncertainty, positioning errors of the tables have been measured few times over one revolution. An exemplary characteristic obtained for the movable table is presented in Fig. 7.

The positioning errors have been determined as the difference between the real angular position of the table top (indicated by the attached angle transducer) and the position calculated according to the number of nominal steps (i.e. 1.2′) performed by the table.

During the tests it has been found out that the maximal error of a single step of the table (defined as a difference between the nominal step and the real one) did not exceed 3 seconds arc. However, it had been discovered that the plays between the worm and the wormwheel were of ca. 5 minutes arc, what had proven the necessity of eliminating them (the plays were completely eliminated in both tables afterwards).

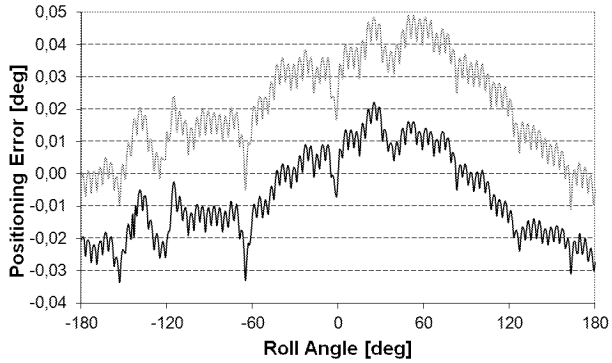

Fig.7: Diagram of the positioning error of the movable table

On the diagram, there are drawn two characteristics of the table, obtained for both directions of its rotation. The noticeable shift between the characteristics results from small plays (that cannot be eliminated) appearing while changing the direction of rotation. Since during a standard operation of the tables only one direction of rotation is used (in order to avoid the hysteresis), further considerations have been limited to the characteristics corresponding to the accepted direction of rotation (lower characteristic in Fig. 7 in the case of the moveable table).

In the case of using only one direction of rotation, the interval between the minimal and the maximal value of the positioning error for the movable table has not exceeded $\pm 0.03^\circ$ ($1.8'$). In the case of the stationary table, it has reached a value of $\pm 0.04^\circ$ ($2.4'$).

4.4. Compensation for the systematic component of the positioning error of the tables

As can be observed in Fig. 7, course of the positioning error has both a systematic as well as a random component. Owing to the fact that each table has been equipped with a sensor of initial position, it is possible to compensate for the systematic component. Therefore, while using diagrams of the positioning error of the tables determined beforehand, it is possible to evaluate a relation between the angular position of the table and the corresponding value of the positioning error.

The course of the positioning error of both tables has been approximated with a polynomial of the fourth order (coefficients of higher orders were statistically insignificant). In the case of the stationary table, the following equation has been obtained:

$$\Delta\alpha = -5{\times}10^{-3} - 2.4{\times}10^{-4}\,\alpha + 5.2{\times}10^{-6}\,\alpha^2 + 1{\times}10^{-8}\,\alpha^3 - 1{\times}10^{-10}\,\alpha^4 \ . \qquad (12)$$

The above regression featured the adjusted R-squared coefficient of 97 % and all the other coefficients significant at the confidence level of $p = 99\,\%$. While regarding Eq. (12), the interval between the extreme values of the compensated positioning error of the table has diminished from $\pm 0.04^\circ$ to $\pm 0.01^\circ$ ($0.6'$). Accepting as previously [see Eq. (10)–(11)] a uniform distribution of possible values of this random component of the positioning error, the respective expanded uncertainty at the confidence level $p = 99\,\%$ will equal $\pm 0.01^\circ$ ($0.6'$).

Analogous polynomial related to the movable table has the following form:

$$\Delta\gamma = 7.3{\times}10^{-3} + 1.2{\times}10^{-4}\,\gamma - 1.8{\times}10^{-6}\,\gamma^2 - 5.6{\times}10^{-9}\,\gamma^3 + 2.3{\times}10^{-11}\,\gamma^4 \ . \qquad (13)$$

The above regression featured the adjusted R-squared coefficient of 78 % and, as previously, all the other coefficients significant at the confidence level of $p = 99\,\%$. Owing to Eq. (13), the interval between the extreme values of the compensated positioning error of the table has been reduced from $\pm 0.03^\circ$ to $\pm 0.02^\circ$ ($1.2'$). So, for a uniform distribution of possible values of this random component of the positioning error, the respective expanded uncertainty at the confidence level $p = 99\,\%$ will equal $\pm 0.02^\circ$ ($1.2'$).

It may be presumed that value of the uncertainty related to the movable table is two times lower than in the case of the stationary table, because of a lower accuracy of the coupling applied while determining its positioning errors.

As uncertainties related to the tables are different, the previous assumption expressed by Eq. (8) is not fully justified, since $2\,u(\alpha) = u(\gamma)$. Taking this into consideration, Eq. (9) must be rearranged as follows:

$$u_{\mathrm{c}}(\beta) = u(\gamma)\sqrt{\frac{\cos^2\alpha\,\cos^2\gamma + 0.25\,\sin^2\alpha\,\sin^2\gamma}{1 - \cos^2\alpha\,\sin^2\gamma}} \tag{14}$$

Having compared Eq. (9) and (14), it can be stated that the maximal value of the combined uncertainty is the same in both cases – the calculated uncertainty does not exceed value of the uncertainty related to operation of the moveable table, i.e. $u(\gamma) = 0.02^\circ$. So, finally the uncertainty of applying the roll is $u_{\mathrm{c}}(\beta)_{\max} = u(\gamma) = 0.02^\circ$.

5. Experimental results

Accuracy of the results obtained during experimental studies depends not only on the test rig itself but also on a methodology employed. The most important issue before starting the experiments is that the tested sensor must be properly fixed in the test rig, aligning its sensitive axes with the respective rotation axes of the test rig [30]–[32]. In order to do it effectively, a special compliant holder was designed, in which the tested senor was mounted.

Another interesting approach has been introduced in [33], where the misalignment errors of a roughly aligned accelerometer, represented by two deviation angles for each of its sensitive axes, have been introduced in respective equations. Then, values of the errors have been determined experimentally, using the method of least squares. In this way the laborious aligning process has been eliminated. As reported in [33], the errors resulted from misalignment and calibration were of ca. 2°. However, uncertainties of the determined misalignments have been not reported, so it is hard to evaluate effectiveness of such approach.

It must not be neglected that the experimental studies are to be performed under strictly defined conditions, mainly with respect to the ambient temperature, since tilt sensors based on MEMS technology are very sensitive to this factor [34]–[36].

The referred experimental studies are carried out mainly in order to calibrate the tested sensor. As already mentioned in the text, there have been proposed some calibration methods, where no test rig is necessary, described e.g. in [37]–[38]. However, in such a case the accuracy of the sensor, influenced by the calibration process [36], is substantially lower.

Apart from calibrating the tested sensors, the test rig allows their accuracy to be estimated. An illustration of such evaluation, based on results obtained during a calibration process of a tilt sensor built of two dual-axis MEMS accelerometers ADXL 202E described in [36], is shown in Fig. 8. The calibration allowed individual values of the accelerometer

offsets and the gains to be determined, and thus the component gravity accelerations to be computed. With accordance to [24], the accuracy of the tested sensor can be estimated with the error expressed over axis y, which has been defined as an absolute value of the difference between the roll angle applied by means of the rotary tables (determined with Eq. (5)) and a corresponding value resulting from an average of respective indications of the tested sensor, measured by means of the data acquisition card, and computed according to rearranged Eq. (2) (black course):

$$e_{(2)} = \left| \beta - \arcsin \frac{g_{\mathrm{y}}}{g} \right| \tag{15}$$

and rearranged and simplified Eq. (3) (gray course):

$$e_{(3)} = \left| \beta - \arccos \frac{g_{\mathrm{z}}}{g} \right| \ . \tag{16}$$

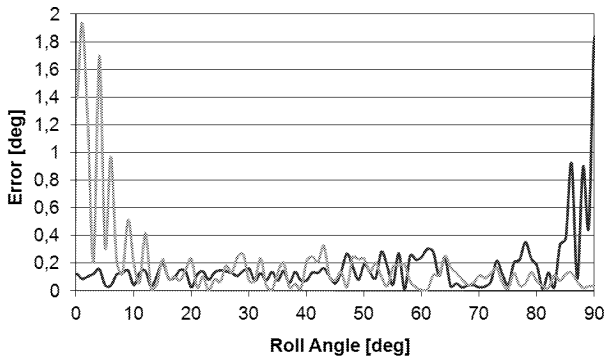

Fig.8: Exemplary results of the experimental studies

In order to evaluate accuracy of the tested accelerometers, let us consider the results corresponding to the range where accelerometers indications are approximately linear, i.e. roll angles within the interval of $\langle 0°; 30° \rangle$ for the black course and $\langle 70°; 90° \rangle$ for the gray course [rapid increase of the respective errors at both ends of the graph results from non-linear character of the relations between the roll and the component accelerations – see Eq. (2) and (3)]. As can be observed, the errors of determining the roll did not exceed 0.2° within the range of quasi-linearity. With regard to the respective catalog datasheet [3], error of the accelerometer indications resulting only from the noise would exceed 0.3°, while the reported cross-axis sensitivity would increase it by 1.8°. So, the obtained results revealed that evaluated accuracy of the tested accelerometers was much better compare to the one resulting from the data provided in the relevant catalog, or evaluated by other researchers, e.g. in [35].

6. Conclusions

At the confidence level $p = 99\,\%$, the presented dual-axis test rig can be characterized by the following features:

– measurements of the analog output voltages of a tested sensor with maximal uncertainty of 0.0016 V,

– application of roll with uncertainty of 1.2 minute arc (±0.02°) over 360°,
– application of pitch with uncertainty of 1.5 seconds arc (±0.0004°) over 360° (or ±0.01° in open loop configuration).

All the above values of uncertainties are low enough for testing tilt sensors based on MEMS accelerometers. More precise tilt sensors can be tested using only one axis of the rig, which allows the pitch angles to be applied with uncertainty of 1.5 seconds arc.

Results of the tests conducted on the rig proved that it is possible to obtain accuracy of tilt sensing of ca. 0.2° in the case of using MEMS accelerometers (provided a constant temperature of the sensor is maintained), what is an evident progress with respect to the values that have been reported hitherto. In the light of the above, it can be stated that performing experimental studies on MEMS accelerometers is one of the most effective ways of improving their performance. Such approach has been not only employed in research practice, but also implemented commercially, e.g. in the case of a triaxial accelerometer presented in [8], where testing of each individual sensor had made it possible to compensate for the offset, gain, cross-axis sensitivity and misalignment of each sensitive axis, and thus its accuracy was significantly improved.

The presented results of experimental works are related to measurements of tilt. However, the test rig is also useful for some studies of low-g accelerometers, where the gravitational acceleration is used as the reference source. A significant advantage of such reference is the fact that it is the most stable, accurate and convenient external reference source available [3], [39]. A corresponding calibration method is commonly used and has been referred to e.g. in [1]–[6], [21]–[22], [30]–[32], [36], [40]. However, it must be realized that it involves the phenomenon of cross-axis sensitivity (having a systematic character). So, when no cross-axis sensitivity is allowed, other methods must be applied, e.g. finding only two extreme values of the output signals and calculating the offset and the gain on this basis, as proposed e.g. in [3]–[6], [16]. Appropriate experiments make it possible to determine values of metrological features of the tested sensors like: accuracy, cross-axis sensitivity, misalignment of the sensitive axes, linearity, sensitivity, offset voltage, gain, and other statistical parameters as well as change of the performance characteristic due to aging.

Additionally, after appropriate modifications, the presented test rig can be used for realization of other research tasks (e.g. experimental studies of kinematic accuracy of couplings or other mechanical units, experimental studies of angular position sensors).

Finally, it is worth mentioning that the introduced test rig is quite simple, and thus inexpensive. At the same time, its performance is comparable with the one of professional solutions presented e.g. in [19], as far as e.g. uncertainty of applying pitch of the tested sensor is concerned.

References

[1] Łuczak S, Beißner S., Büttgenbach S.: Tilt Sensor Based on a 3-Axis MEMS Accelerometer, in: Conf. Automation 2003, Warsaw, Poland 2003, pp. 271–280
[2] Bütefisch S., Schoft A., Büttgenbach S.: Three-Axes Monolithic Silicon Low-g Accelerometer, J. Microelectromech. Syst. (2000) vol. 9, no. 4, pp. 551–556
[3] Low Cost ±2g Dual Axis Accelerometer with Duty Cycle Output, ADXL 202E, Analog Devices Inc., Norwood, MA 2000
[4] Low Cost ±1.2g Dual Axis Accelerometer, ADXL 213, Analog Devices Inc., Norwood, MA 2004

[5] Small and Thin ±2g Accelerometer, ADXL 322, Analog Devices Inc., Norwood, MA 2005
[6] Precision ±1.7g Single/Dual Axis Accelerometer ADXL 103/ADXL 203, Analog Devices Inc., Norwood, MA 2005
[7] Ultra Low Cost, ±1.0 g Dual Axis Accelerometer with Absolute Outputs MXA2500J/K, MEMSIC Inc., North Andover, MA 2006
[8] AX301 Three-Axis Accelerometer Module, Preliminary Specifications, Sentera Technology Corporation, Berkeley, CA 2003
[9] Čech V., Jevický J.: Generator of Command Signals for Testing Servomechanisms of Pan and Tilt Devices, Eng. Mech. (2011) vol. 18, no. 5/6, pp. 331–340
[10] Knapp G.S., You H., Holzhausen G.R.: On the use of electronic tilt sensors as angle encoders for synchrotron applications, Rev. Sci. Instr. (1995) vol. 66, no. 2, pt. 2, pp. 1712–1714
[11] Baltag O., Costandache D., Salceanu A.: Tilt Measurement Sensor, Sensors & Actuators (2000) vol. A 81, no. 1–3, pp. 336–339
[12] Acar C., Shkel A.: Experimental evaluation and comparative analysis of commercial variable-capacitance MEMS accelerometers, J. Micromech. Microeng. (2003) vol. 13, no. 5, pp. 634–645
[13] Won S.P., Golnaraghi F.: A Triaxial Accelerometer Calibration Method Using a Mathematical Model, IEEE Trans. Instr. Meas. (2010) vol. 59, no. 8, pp. 2144–2153
[14] Yun S.S., Jeong D.H., Wang S.M., Je C.H., Lee M.L., Hwang G., Choi C.A., Lee J.H.: Fabrication of morphological defect-free vertical electrodes using a (1 1 0) silicon-on-patterned-insulator process for micromachined capacitive inclinometers, J. Micromech. Microeng. (2009) vol. 19, doi 035025
[15] Qian J., Fang B., Yang W., Luan X., Nan H.: Accurate Tilt Sensing with Linear Model, IEEE Sensors J. (2011) vol. 11, no. 10, pp. 2301–2309
[16] Ang W.T., Khosla P.K., Riviere C.N.: Nonlinear regression model of a low-g MEMS accelerometer, IEEE Sensors J. (2007) vol. 7, no. 1, pp. 81–88
[17] Latt W.T., Veluvolu K.C., Ang W.T.: Drift-Free Position Estimation of Periodic or Quasi-Periodic Motion using Inertial Sensors, Sensors-Basel (2011) vol. 11, doi 5931–5951
[18] Kibrick R., Robinson L., Cowley D.: An evaluation of precision tilt-sensors for measuring telescope position, in: Telescope Contr. Syst., SPIE Symposium on OE/Aerosp. Sensing and Dual Use Photon., Orlando, FL 1995, pp. 364–376
[19] Automatic Positioning And Rate Test Tables (1530 Series), Ideal Aerosmith Inc., East Grand Forks, MN 2003
[20] Oleksiuk W., Czerwiec W., Munerato F., Mihalachi D., Laurent C., Nitu C., Comeaga C.D.: Flexible MiniůRobot with Autonomous Motion, in: ICRAM'99, Istanbul, Turkey 1999, pp. 396–401
[21] Łuczak S.: Standard MEMS Accelerometer as a Dual-Axis Tilt Sensor, in: 47th Internationales Wissenschaftliches Kolloquim, Ilmenau, Germany 2002, pp. 244–245
[22] Łuczak S.: Test Station for Studying Miniature Tilt Sensors, in: Int. Conf. Mechatronics 2000, Warsaw, Poland 2000, vol. 1, pp. 253–256
[23] Popowski S.: Wyznaczanie kąta pochylenia i przechylenia w tanich systemach nawigacji lądowej, J. Aeronautica Integra (2008) no. 1/2008 (3), pp. 93–97 (in Polish)
[24] Łuczak S., Oleksiuk W., Bodnicki M.: Sensing Tilt with MEMS Accelerometers, IEEE Sensors J. (2006) vol. 6, no. 6, pp. 1669–1675
[25] Guide to the Expression of Uncertainty in Measurement, 1st ed., International Organization for Standardization, Geneva, Switzerland 1993, pp. 13, 19, 54, 59
[26] PC-LabCard PCL-818 L High-performance Low Cost Data Acquisition Card. User's Manual, Advantech Co., Ltd., Taipei, Taiwan 1995
[27] Mościcki W., Czerwiec W.: Testing Kinematic Accuracy of Miniature Couplings, in: III Conf. Mechatronika '97, Warsaw, Poland 1997, Prace naukowe, Konferencje, vol. 14, pp. 547–552 (in Polish)
[28] Łuczak S., Czerwiec W., Mościcki W.: Kinematic Accuracy of Miniature Couplings, Pomiary, Automatyka, Robotyka (2006) vol. 2/2006, pp. 12–15 (in Polish)
[29] IDW Incremental Transillumination Angle-Measuring System, Jenoptik Carl Zeiss JENA GmbH, Berlin/Leipzig, Germany 1989

[30] Łuczak S.: Experimental Studies of Miniature Tilt Sensors, Elektronika (2004) no. 8–9/2004, pp. 215–218
[31] Chen H., Bao M., Zhu H., Shen S.: A piezoresistive accelerometer with a novel vertical beam structure, Sensors & Actuators (1997) vol. A 63, pp. 19–25
[32] Low g Accelerometer Non-Linearity Measurement, #AN-00MX-014 Application Note n/r 5/12/03, MEMSIC Inc., North Andover, MA 2005
[33] Parsa K., Lasky T. A., Ravani B.: Design and Implementation of a Mechatronic, All-Accelerometer Inertial Measurement Unit, IEEE/ASME Trans. Mechatr. (2007) vol. 12, no. 6, pp. 640–650
[34] Reducing Accelerometer Temperature Drift with Crystal Ovens, Sensors (1996) vol. 13, no. 4, p. 92
[35] Horton M., Kitchin C.: A Dual Axis Tilt Sensor Based on Micromachined Accelerometers, Sensors (1996) vol. 13, no. 4, pp. 91–94
[36] Łuczak S.: On Improving Performance of MEMS Accelerometers in Tilt Sensing, Machine Dynamics Problems (2006) vol. 30, no. 4, pp. 37–47
[37] Šipoš M., Pačes P., Roháč, J., Nováček, P.: Analyses of triaxial accelerometer calibration algorithms IEEE Sensors J. (2012) vol. 12, no. 5, pp. 1157–1165
[38] Frosio I.; Pedersini F., Borghese N.A.: Autocalibration of Triaxial MEMS Accelerometers With Automatic Sensor Model Selection, IEEE Sensors J. (2012) vol. 12, no. 6, pp. 2100–2108
[39] Model 900 Biaxial Clinometer Data Sheet, Applied Geomechanics, Santa Cruz, CA 1995
[40] Sensors & Sensory Systems Catalog, Crossbow, San Jose, CA 2006, pp. 61–71

Received in editor's office: December 6, 2012
Approved for publishing: January 3, 2013